Manipulation Analysis of Two Cooperating Arms

N. M. Fonseca Ferreira

Dep. of Electrical Engineering
Institute of Engineering of Coimbra
Quinta da Nora
3031-601 Coimbra Codex, Portugal
email: nunomig@isec.pt

J. A. Tenreiro Machado

Dep. of Electrical Engineering
Institute of Engineering of Porto
Rua Dr António Bernardino de Almeida
4200-072 Porto Codex, Portugal
email: jtm@dee.isep.ipp.pt

Abstract

Many tasks involving manipulation require cooperation between robots. Meanwhile, it is necessary to determinate the adequate values for the robot parameters to obtain a good performance. This paper discusses several aspects related with the manipulability and the workspace of two co-operative robots when handling objects with different lengths and orientations.

1. Introduction

The choice of a robotic mechanism depends on the task or the type of work to be performed and, consequently, is determined by the position of the robots and by their dimensions and structure. In general, the selection is done through experience and intuition; nevertheless, it is important to measure the manipulation capability of the robotic system [1], what can be useful in the robot control and in the task planning. In this perspective it was proposed the concept of kinematic manipulability measure [2] and its generalization dynamical manipulability [3-4] or, alternatively, to a statistical evaluation of manipulation [5-6]. Moreover, other related aspects such as the coordination of two robots handling objects, collision avoidance and free path planning have been also investigated [7-12] but still require further study.

This paper analyses the manipulation measure and capability of two–arm systems using a numerical technique. Bearing these facts in mind, this article is organized as follows. Section two, develops a numerical method for analyzing the manipulability of robotic systems. Based on the new algorithm, sections three and four study the performance and the workspace of two–arm systems, respectively. Finally, section five outlines the main conclusions.

2. Manipulability of Robotic Systems

The manipulability measures the robot efficiency in the workspace from the viewpoint of object manipulation. For one arm the kinematic manipulability μ is defined as:

$$\mu = |\det[\boldsymbol{J}(\mathbf{q})\boldsymbol{J}^T(\mathbf{q})]|^{1/2} \qquad (1)$$

where $\boldsymbol{J}$ is Jacobian of the robot kinematics. With this formulation, for example, the *RR* robot it characterized by $\mu = l_1 l_2 |\sin(q_2)|$, where l_i and q_i $(i = 1,2)$ are the length and position of link i, respectively. Based on this expression we can verify that the best posture for the *RR* robot occurs when $q_2 = \pm 90°$ and, for a total length $l_1 + l_2 = L$, μ has a maximum when $l_1 = l_2$.

For one robot the analytical development of μ is straightforward; however, for two or more robots the definition of μ is more complex. To overcome this problem we adopt a numerical approach inspired by the Monte Carlo method. In this perspective, we analyze both methods for a single robot, with the purpose of comparing the numerical algorithm and the classical expression (1) and then we extend the concept for two robots working in cooperation.

For a k-dof manipulating structure, the new method [13] consists in generating a numerical random sample of n points inside a sphere with radius ρ (Fig. 1), in the joint space with center at $(q_{1c},\ldots,q_{kc})$, and to map them through the direct kinematics to the operational space, in order to obtain a set of points corresponding to an ellipsoid with center at (x_c,y_c). The size and shape of each ellipsoid determine the "amplification" between the joint space and the operational space. The amplification is related to eigenvalues of the Jacobian and corresponds to the area of the ellipsoid.

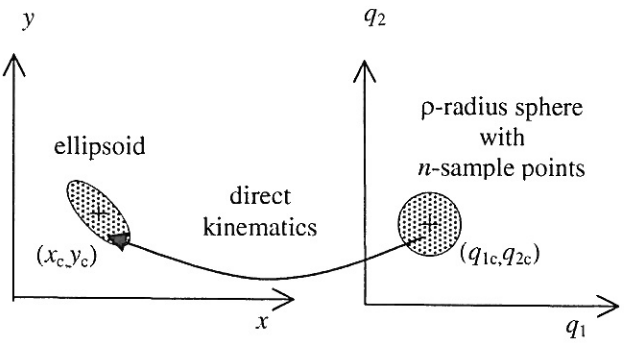

Fig. 1 – Manipulability analysis through the numerical method.

The manipulability varies in the workspace W and, in order to analyze its texture, we establish a grid of m points for the centers of the sphere → ellipsoid transformation. Therefore, we consider some sub-indices to simplify the study of the manipulability of several arms. By other words, to condense the information we define:

• The sub-index μ_1 as the maximum value of μ, in all the possible workspace W.

$$\mu_1 = Max\ [\ \mu(x,y), \forall\ (x,y) \in W\ ] \qquad (2)$$

• The sub-index μ_2 as the average volume of μ considering only the workspace W where $\mu \neq 0$.

$$\mu_2 = Av\ [\ \mu(x,y), \forall\ (x,y) \in W: \mu(x,y) \neq 0\ ] \qquad (3)$$

• The index μ_3 as average volume of μ, in all the possible workspace W.

$$\mu_3 = Av\ [\ \mu(x,y), \forall\ (x,y) \in W\ ] \qquad (4)$$

3. Manipulability: A Numerical Approach

The following experiments adopt one and two robots with RR structure. In a first phase we consider a single robot, in order to compare the analytical and numerical methods. In a second phase, we consider two robots working in cooperation (figure 2), in order to determinate the manipulability of the total system and the system configuration that leads to a superior performance.

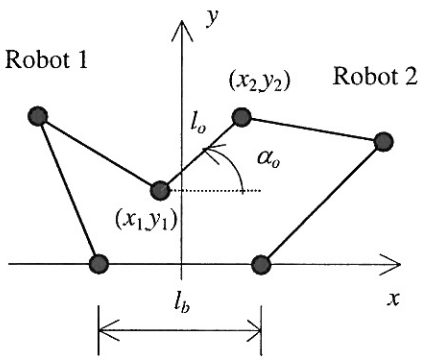

Fig. 2 - Two RR robots working in cooperation for the manipulation of an object with length l_o, orientation α_o and distance l_b between the shoulders.

3.1. Manipulability of One Robot

Figures 3 shows the manipulability for one RR robot in the workspace obtained by the two alternative methods we verify that the numerical method presents a small error when compared with the analytical expression. Furthermore, the new algorithm has a low computational cost and it is easy to implement. Obviously, to decrease the numerical error it is necessary to increase n of samples, but the calculation time increases proportionally.

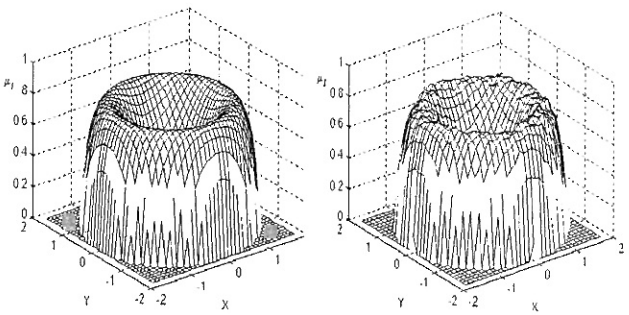

a) b)

Fig. 3 - Manipulability μ of one RR robot with $l_1 = 1$ m and $l_2 = 0.8$ m obtained by the: a) analytical method, b) numerical algorithm for a sample of $n = 1000$ points and a grid of $m = 1000$ points.

3.2. Manipulability of Two Robots

In this sub-section, we consider two robots working in cooperation. In this way, we start with several experiments to obtain the manipulability of the two arms in its workspace for $l_o = 0$ (small objects) and $l_b \in [0, 2(l_1 + l_2)]$. Given the kinematic redundancy of the two-arm system, for each grasping point we consider that, the left and the right arms define, alternatively, the hand position.

Figure 4 shows the sub-index μ_1 in the workspace of two RR robots working in cooperation for $l_b \in [0, 4[$ and the cases $A = \{l_1 = 0.5,\ l_2 = 1.5\}$, $B = \{l_1 = 1.5,\ l_2 = 0.5\}$, $C = \{l_1 = 1,\ l_2 = 1\}$. The chart shows μ_1 versus l_b, the distance between the arm elbows, and reveals that we obtain larger values for $l_b \approx 0$ because the workspace is maximum in that case, while the best case occurs for $l_1 = l_2$

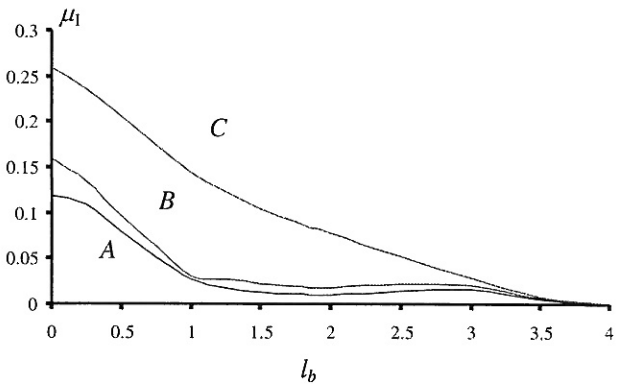

Fig. 4 – Manipulability sub-index μ_1 for $A = \{l_1 = 0.5,\ l_2 = 1.5\}$, $B = \{l_1 = 1.5,\ l_2 = 0.5\}$, $C = \{l_1 = 1,\ l_2 = 1\}$.

Therefore, we can say that, when manipulating small objects, the distance between the arms should be $l_b = 0$, for arms having $l_1 = l_2 = 1/2\ L$, with $L = 2$ m. Nevertheless, studying the human body we see that it presents $l_1 = l_2$ and $1/2\ L < l_b < 3/2\ L$. Therefore, the parameters l_o and α_o must influence the manipulability and this hypothesis must be investigated. In this line of thought, we consider for the first study two identical RR robots with $l_1 = l_2$ cooperating in the manipulation of

objects with dimension $l_o = \{0,2,4\}$ while varying $l_b \in [0, 2(l_1+l_2) + l_o]$ and $\alpha_o \in [-180°, +180°[$.

Figures 5–7 show the sub-indices μ_1, μ_2 and μ_3 versus the parameters l_o, l_b and α_o for two *RR* robots. This numerical experiment considers a grid of $m = 1000$ points and, for each of these points, a sample of $n = 1000$ points, inside a sphere with a radius of $\rho = 0.1$ rad in the joint space. Figure 8 shows the relationship between the length l_o and the distance between the arms l_b for $\alpha_0 = 0$. We can observe that we get a maximum manipulability for $l_o = l_b$.

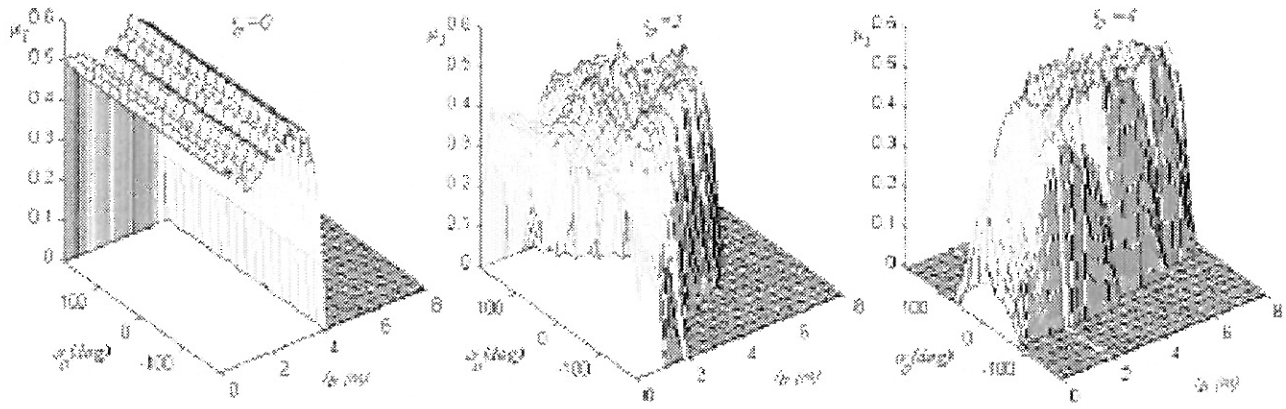

Fig. 5 – Two arm maximum manipulability μ_1 versus l_b and α_o for object lengths $l_o = \{0, 2, 4\}$, with $m = 1000$, $n = 1000$, $\rho = 0.1$ rad, *RR*-Robots 1 and 2: $\{l_1 = l_2 = 1$ m$\}$.

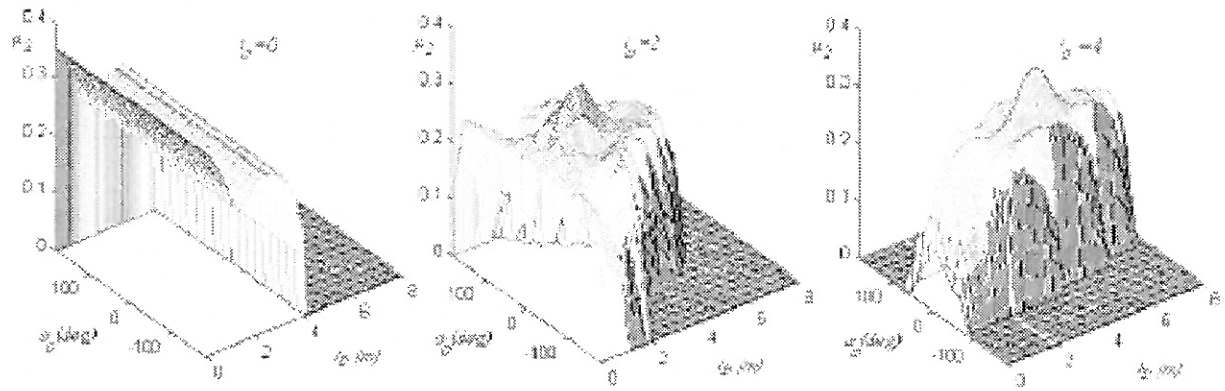

Fig. 6 – Two arm average volume of the manipulability μ_2 versus l_b and α_o for object lengths $l_o = \{0, 2, 4\}$, with $m = 1000$, $n = 1000$, $\rho = 0.1$ rad, *RR*-Robots 1 and 2: $\{l_1 = l_2 = 1$ m$\}$.

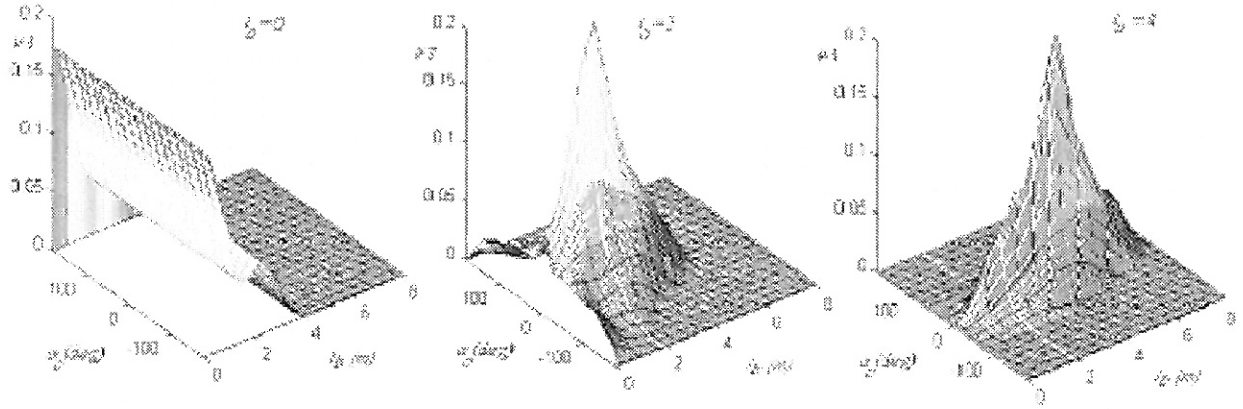

Fig. 7 – Two average manipulability for the considered basis μ_3 versus l_b and α_o for object lengths $l_o = \{0, 2, 4\}$, with $m = 1000$, $n = 1000$, $\rho = 0.1$ rad, *RR*-Robots 1 and 2: $\{l_1 = l_2 = 1$ m$\}$.

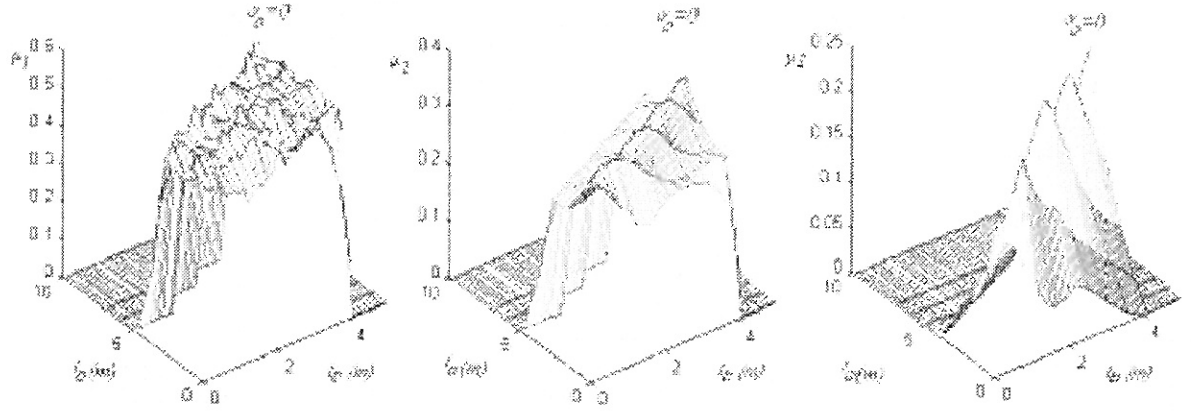

Fig. 8 – The sub-indices of manipulability μ_1, μ_2 and μ_3 versus $l_o \in [0, 10]$ and $l_b \in [0, 5]$, for an object orientation $\alpha_o = 0$, $m = 1000$, $n = 1000$, $\rho = 0.1$ rad, *RR*-Robots 1 and 2:$\{l_1 = l_2 = 1$ m$\}$.

4. Workspace Analysis

In this section we analyze another important aspect of robot co-operation, namely the system workspace and its properties. In this line of thought, we compare the workspace for experiments having distinct robot joint-angle limits (q_{imax} and q_{imin}, $i = 1, 2$) and several distances l_b between the robots.

For large values of l_b, required in the body for handling large objects, the workspace is just a small 'ellipse', without holes, because the robots are so separated apart that it is impossible to have contacts between them and/or the object. Nevertheless, this situation is far from the case of the human body and, therefore, in our experiments we will consider the case of $l_b \leq l_1+l_2+l_0$, $l_o = l_b = 1$ and $\alpha_o = 0$.

For comparison, the first experiment depicts the workspace of two *RR* arms with no limitations on the robot joints (Table 1) while the second and third experiments consider the joints limitations of Tables 2 and 3, respectively. Figures 9 to 11 show the corresponding workspace and manipulability.

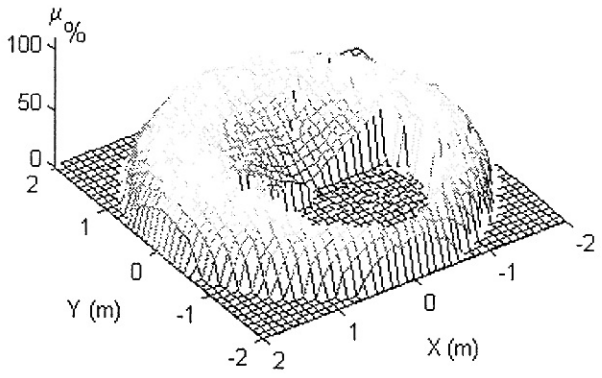

Fig. 9 – Two *RR*-arm manipulability μ and workspace for $\alpha_o = 0$, $l_o = l_b = 1$, $m = 1000$, $n = 1000$, *RR*-Robots 1 and 2 $\{l_1 = l_2 = 1$ m$\}$ and the joint angle limitations of Table 1.

Table 1 – Two *RR* arm system without joint limitations

Robot	q_{1min} (rad)	q_{1max} (rad)	q_{2min} (rad)	q_{2max} (rad)
1	$-\pi$	π	$-\pi$	π
2	$-\pi$	0	0	π

Table 2 – Two *RR* arm system with light joint limitations

Robot	q_{1min} (rad)	q_{1max} (rad)	q_{2min} (rad)	q_{2max} (rad)
1	0	π	0	π
2	$-\pi$	0	0	π

Figure 9 shows an "hole" in the lower side of the workspace that is due to the chock between the object and the two arms. Moreover, the chart reveals that the region of the maximum manipulability in the operational workspace is in the same place as the one shown in the single arm case. On the other hand, Figures 10-11 show that the diminishing of the workspace is due to the joint angle limitations.

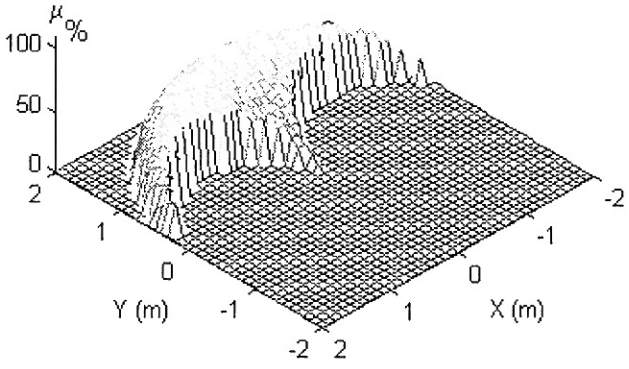

Fig. 10 – Two *RR*-arm manipulability μ and workspace for $\alpha_o = 0$, $l_o = l_b = 1$, $m = 1000$, $n = 1000$, *RR*-Robot 1 and 2: $\{l_1 = l_2 = 1$ m$\}$ and the joint angle limitations of Table 2.

Table 3- Two *RR* arm system with strong joint limitations

Robot	q_{1min} (rad)	q_{1max} (rad)	q_{2min} (rad)	q_{2max} (rad)
1	0	π	0	π
2	$-8/9\ \pi$	0	0	$8/9\ \pi$

Note that the third experience considers joints limitations that resemble the human arm case. However, if we study the human body and the manipulation through two arms we observe that it is not 'prepared' to manipulate very large objects. In fact, our arms have a good working region near the body and, as we shall see, superior than the case of two *RR* mechanical arms. Consequently, to improve the workspace properties the system must have cooperative robots with kinematic redundancy [14].

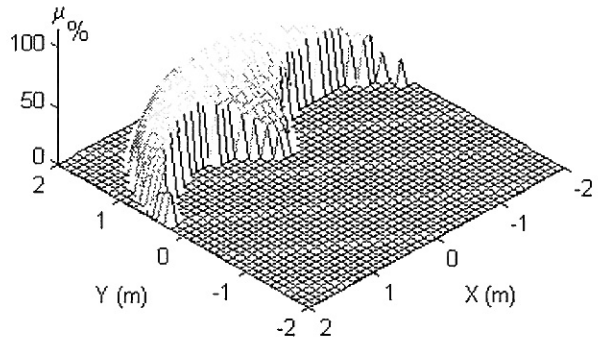

Fig. 11 – Two *RR*-arm manipulability μ and workspace for $\alpha_o = 0$, $l_o = l_b = 1$, $m = 1000$, $n = 1000$, *RR*-Robots 1 and 2: $\{l_1 = l_2 = 1$ m$\}$ and the joint angle limitations of Table 3.

In this perspective we adopt two *RRR* co-operating arms so that the total length of each arm remains $L = 2$ m for the two cases *i*) $l_1 = l_2 = l_3 = 2/3$ m and *ii*) $l_1 = 5/6$ m, $l_2 = 2/3$ m and $l_3 = 1/2$ m. Moreover, due to the redundancy, there is an infinite number of arm configurations (and, consequently, of values of μ) for each manipulating point (x,y). Therefore, we consider the average manipulability μ_{Av} to captures all manipulation possibilities. By other words, we take the average of μ over the set of al possible robot configurations that lead to the same object location and orientation in the operational space.

Figures 12-13 show μ_{Av} for robots without joint angle limitations (Table 4) when considering the case of $l_o = l_b = 1$ m and $\alpha_o = 0$.

Figures 14-15 show the workspace and the manipulability with joint angle limitations (Table 5) when considering the case of $l_o = l_b = 1$ m and $\alpha_o = 0$.

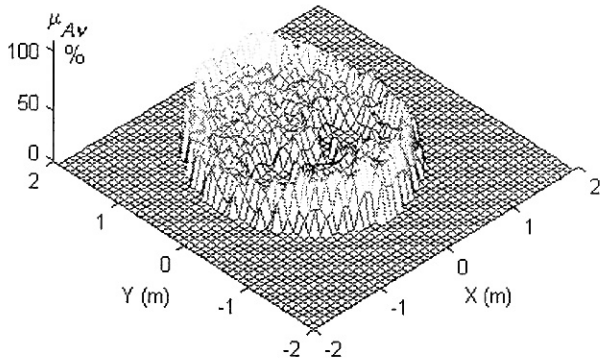

Fig. 12 – Two *RRR*-arm μ_{Av} and workspace for $\alpha_o = 0$, $l_o = l_b = 1$, *RRR*-Robots 1 and 2: $\{l_1 = l_2 = l_3 = 2/3$ m$\}$ and the joint angle limitations of Table 4.

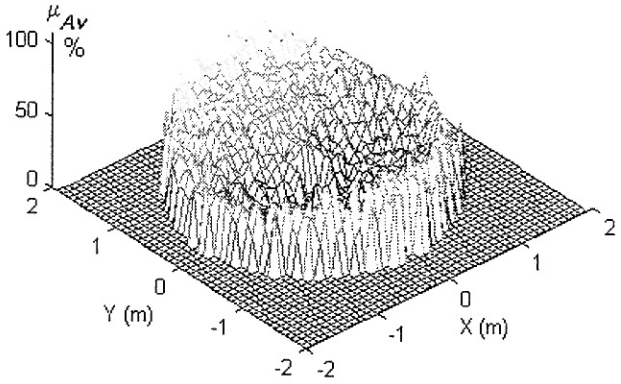

Fig. 13 – Two *RRR*-arm μ_{Av} and workspace for $\alpha_o = 0$, $l_o = l_b = 1$, *RRR*-Robot 1 and 2: $\{l_1 = 5/6$ m, $l_2 = 2/3$ m, $l_3 = 1/2$ m$\}$ and the joint angle limitations of Table 4.

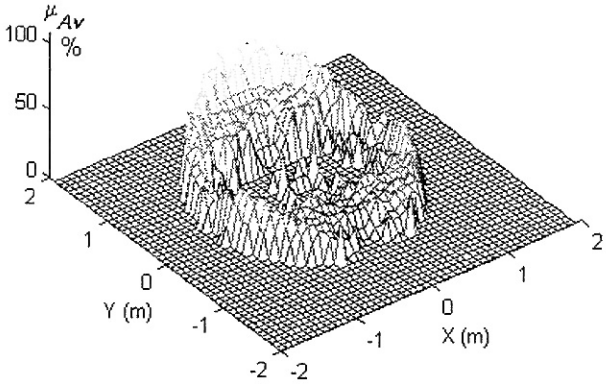

Fig. 14 – Two *RRR*-arm μ_{Av} and workspace for $\alpha_o = 0$, $l_o = l_b = 1$, *RRR*-Robots 1 and 2: $\{l_1 = l_2 = l_3 = 2/3$ m$\}$ and the joint angle limitations of Table 5.

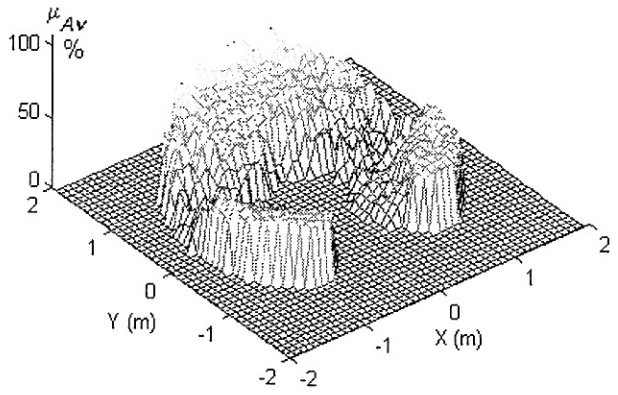

Fig. 15 – Two *RRR*-arm μ_{Av} and workspace for $\alpha_o = 0$, $l_o = l_b = 1$, *RRR*-Robot 1 and 2: $\{l_1 = 5/6$ m, $l_2 = 2/3$ m, $l_3 = 1/2$ m$\}$ and the joint angle limitations of Table 5.

Table 4 – Two *RRR* arm system without joint limitations

Robot	q_{1min} (rad)	q_{1max} (rad)	q_{2min} (rad)	q_{2max} (rad)	q_{3min} (rad)	q_{3ax} (rad)
1	$-\pi$	π	$-\pi$	π	$-\pi/2$	$\pi/2$
2	$-\pi$	π	$-\pi$	π	$-\pi/2$	$\pi/2$

Table 5 – Two *RRR* arm system with joint limitations

Robot	q_{1min} (rad)	q_{1max} (rad)	q_{2min} (rad)	q_{2max} (rad)	q_{3min} (rad)	q_{3ax} (rad)
1	0	π	$-8/9\,\pi$	$8/9\,\pi$	$-\pi/2$	$\pi/2$
2	0	π	$-8/9\,\pi$	$8/9\,\pi$	$-\pi/2$	$\pi/2$

When considering the joint angle limitations (Table 5) it is straightforward that the kinematic redundancy has improved largely the workspace area. Furthermore, the workspace of case *i*) seems inferior to the case *ii*), namely from the point of view of human manipulation. In fact, the reduction of the work area in the back part of the body is less important than the elimination of the 'hole' revealed in *ii*), near the center-frontal part of the body.

5. Summary and Conclusions

This paper developed a study of the manipulation capability of two robots working in cooperation. In this perspective, a numerical tool was introduced for the analysis of the kinematic manipulability of multiple robots in the workspace. Based on the new algorithm several sub-indices were evaluated in order to characterize the system manipulability. It was possible to compare distinct situations, such as different sizes and orientations of the object and distinct lengths between the two arms. Moreover, the kinematic redundancy and joint angle limitations were also investigated, in order to compare the numerical results and the characteristics of the human being.

References

[1] Y. C. Tsai and A.H Soni, "Accessible Region and Synthesis of Robot Arms," ASME J. Mech. Design, vol. 103, pp. 803-811, Oct. 1981.

[2] T. Yoshikawa, "Manipulability of Robotic Mechanisms," The Int. J. Robotics Research, vol. 4, pp. 3-9, Summer, 1985.

[3] H. Asada, "A Geometrical Representation of Manipulator Dynamics and its Application to Arm Design," ASME J. Dynamic Syst., Meas., Contr., vol. 105, pp. 131-142, 1983.

[4] V. Scheinman and B. Roth, "On the Optimal Selection and Placement of Manipulators," RoManSy'84: The Fifth CISM-IFToMM Symp., Udine, Italy, 1984.

[5] A. M. Galhano, J. M. de Carvalho and J. A. T. Machado, "The Statistical Study of Robot Manipulators," IEEE Int. Symp. on Intelligent Control, Philadelphia, Pennsylvania, USA, 1990.

[6] J. A. T. Machado and A. M. Galhano, "A Statistical and Harmonic Model for Robot Manipulators," IEEE Int. Conf. on Robotics and Automation, Albuquerque, New Mexico, USA, 1997.

[7] Y. P. S. Chien, Q. L. Xue, Y. Chen, "C- Subspace Model of Tightly Coordinated Two-Planar Robots", International Journal of Robotics and Automation, vol. 8, N°1, 1989.

[8] Y. Nakamura, K. Nagai, T. Yoshikawa, "Dynamics and Stability in Coordination of Multiple Robotic Mechanisms," International Journal of Robotics Research, vol. 8, pp. 44-61, 1989.

[9] B. Cao, G. I. Dodds, G. W. Irwin, "An Approach to Time Optimal, Smooth and Collision-Free Path Planning in a Two Robot Arm Environment" International Journal of Robotics, vol. 14, pp 61-70, 1996.

[10] T. J. Tarn, A. K. Bejczy, P. K. De, "Analysis of the Dynamic Ability of Two Robot Arms in Object Handling", Advanced Robotics, vol. 10, n. 3, pp. 301-315, 1996.

[11] C. Y. Kim, Y. S. Yoon, "Task Space Dynamic Analysis for Multi-Arm Robot Using Isotropic Velocity and Acceleration Radii", Int. J. of Robotics, vol. 15, pp. 319-329, 1997.

[12] N. M. Fonseca Ferreira, J. A. Tenreiro Machado, "Manipulability Analysis of Two-Arm Robotic Systems", 4th IEEE International Conference on Intelligent Engineering Systems, Portoroz, Slovenia, Sept. 2000.

[13] A. K. Bejczy and T. Jonhg Tarm, "Redundancy in Robotics Connected Robots Arms as Redundant Systems", 4th IEEE International Conference on Intelligent Engineering Systems, Portoroz, Slovenia, Sept. 2000.

[14] Fernando B. M. Duarte, J. A. Tenreiro Machado, "Chaos Dynamics in the Trajectory Control of Redundant Manipulators", IEEE Int. Conference on Robotics and Automation, San Francisco, USA, April 2000.